Effective rf sheath impedance and implications for sheath power absorption

J. R. Myra

Lodestar Research Corporation, Boulder, CO, USA

November 2016

DOE-ER/54392-84 LRC-16-168

LODESTAR RESEARCH CORPORATION
2400 Central Avenue
Boulder, Colorado 80301

Effective rf sheath impedance and implications for sheath power absorption

J. R. Myra

Lodestar Research Corporation, 2400 Central Avenue, Boulder, Colorado 80301

Abstract

RF sheaths form near surfaces where plasma and strong rf fields coexist. The effect of these rf sheaths on wave propagation near the boundary can be characterized by an effective sheath impedance. [J. R. Myra and D. A. D'Ippolito, Phys. Plasmas **22**, 062507 (2015)] In general the complex sheath impedance includes both resistive and capacitive contributions which describe rf sheath rectification and rf power absorption in the sheath. Here we consider a class of model problems for slow wave interaction with a sheath, and analyze the effect of the complex impedance. For the propagating slow wave case, where the incident wave is partially reflected, the fraction of power dissipated is calculated. For the evanescent slow wave case, which admits a sheath-plasma resonance, it is shown that power is transferred to the sheath by evanescent tunneling, broadening the resonance. Estimates of the rf sheath power dissipation per unit are given.

Keywords: ICR heating, Plasma sheaths, Plasma confinement | Magnetic confinement | Tokamaks

I. Introduction

The application of rf power in the ion cyclotron range of frequencies (ICRF) is important in magnetic fusion experiments, especially for heating and current drive in tokamaks approaching the reactor regime. The key physics issue facing ICRF is in the interaction of these rf waves with plasma in the vicinity of material surfaces. Here the waves can drive rf sheaths, and these sheaths can produce a number of unwanted interactions such as rf-enhanced impurity sputtering and self-sputtering, both global and local parasitic power dissipation, with the latter admitting the possibility of material damage or accelerated erosion. Reviews of experimental and theoretical work on ICRF edge and wall interactions are given in Refs. 1-2 and a short overview of the physics can be found in Ref. 3. More recently, these issues have been the subject of experimental investigations on many tokamaks,[4-11] and have given rise to a number of dedicated modeling efforts.[12-19]

The need to facilitate modeling of ICRF sheath interactions in global rf codes has given rise to the development of a sheath boundary condition (BC)[20] at the sheath-plasma interface. The sheath BC is an extension of the metal wall BC to include the effect of sheath capacitance in the narrow Debye scale layer. (A similar BC was developed for simulations of plasma processing in Ref. 21.) Recently the capacitive sheath BC was generalized to include the effects of particle as well as displacement currents, giving rise to a complex sheath impedance (with resistive and capacitive parts).[22] The generalized sheath model is also appropriate for describing oblique angle rf sheaths with fully or partially magnetized ions.

In this report, some of the properties of the generalized sheath BC are illustrated; specifically matching of ICRF waves to the impedance BC are explored with attention implications for the sheath-plasma resonance and for rf power absorption by the sheath. Although rf sheaths can result from both incident fast waves (FW) and slow waves (SW), the $E_{||}$ component of the SW is almost entirely responsible for the development of the rf sheath. Consequently, this investigation will focus on the SW for which the $E_{||}$ component is intrinsically the largest. Furthermore, as an analytical simplification, the case where the background magnetic field is perpendicular to the wall is considered.

II. Model geometry and SW propagation physics

The geometry, shown in Fig. 1, is that of SW propagation (or evanescence) along a magnetic field into a wall.

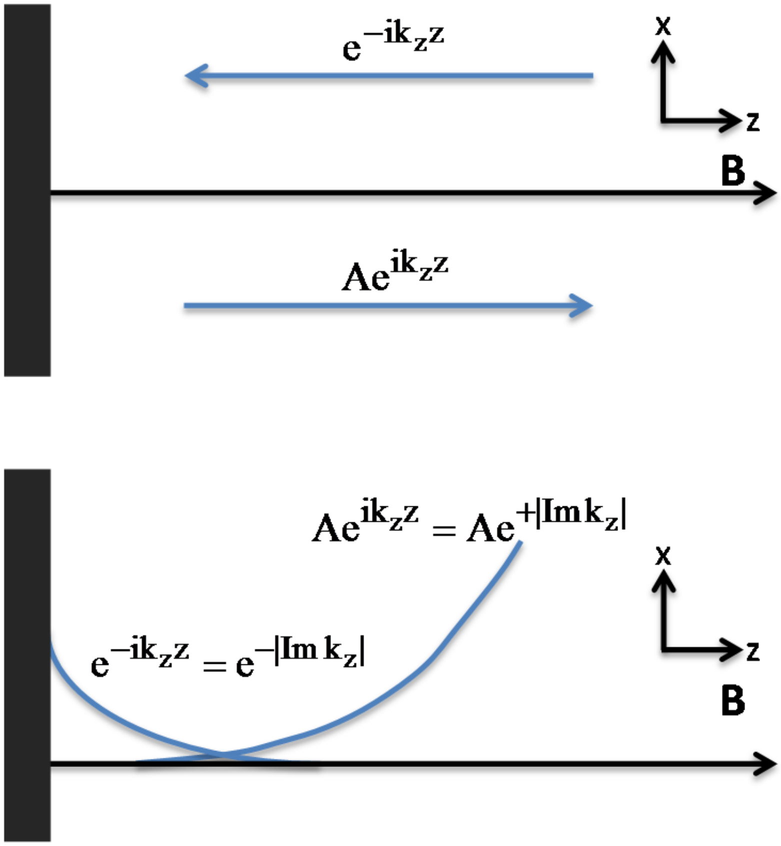

Fig. 1 Upper panel: model geometry show an incoming (left propagating) wave with unit amplitude and a reflected (right propagating) wave with amplitude A. The sheath is at the left and $k_z > 0$. Power is transferred from the incoming wave to the sheath and to the reflected "A-wave". Lower panel: the same geometry for the case where the waves are evanescent. In this case the power is transferred via evanescent tunneling from the "A-wave" to the sheath plasma wave (see Sec. V) where the latter decays away from the left wall. The sign convention is Im $k_z < 0$.

In keeping with standard conventions, the right-propagating wave is assumed to have phase variation ~ $\exp(ik_x x+ik_z z-i\omega t)$ with $k_z > 0$. The magnetic field is oriented in the z-direction, $\mathbf{B} = B\mathbf{e}_z$ and throughout this document, subscripts $\|$ and $\perp$ with respect to $\mathbf{B}$ refer to the x and z directions respectively.

In this geometry, the SW has its electric field polarized in the x and z directions, and for the right-going wave the solution is given by

$$\begin{pmatrix} \varepsilon_\perp - n_z^2 & n_x n_z \\ n_x n_z & \varepsilon_\| - n_x^2 \end{pmatrix} \begin{pmatrix} E_x \\ E_z \end{pmatrix} = 0, \tag{1}$$

where **n** = **k**c/ω,

$$\varepsilon_{\perp} = 1 - \frac{\omega_{pi}^2}{\omega^2 - \Omega_i^2} \tag{2}$$

$$\varepsilon_{||} = 1 - \frac{\omega_{pe}^2}{\omega^2}\,. \tag{3}$$

The total incident plus reflected SW field takes the form

$$\mathbf{E} = \mathbf{e}'_{sw} e^{-ik_z z} + \mathbf{e}_{sw} A e^{ik_z z} \tag{4}$$

where the phase variation in x and t has been suppressed. Here the unit polarization vector of the SW for the right-going wave is

$$\mathbf{e}_{sw} = \frac{(n_x^2 - \varepsilon_{||})\mathbf{e}_x + n_x n_z \mathbf{e}_z}{\left|(n_x^2 - \varepsilon_{||})\mathbf{e}_x + n_x n_z \mathbf{e}_z\right|} \tag{5}$$

For the left-going wave the polarization vector is given by the replacement

$$\mathbf{e}'_{sw}(n_z) = \mathbf{e}_{sw}(-n_z) \tag{6}$$

From Eq. (1) the dispersion relation is obtained as

$$n_x^2 \varepsilon_{\perp} + n_z^2 \varepsilon_{||} = \varepsilon_{\perp}\varepsilon_{||} \tag{7}$$

In this problem we regard ω and k_x as specified input parameters; k_z is to be obtained from the dispersion relation. Here and henceforth we consider plasmas of sufficient density that the one in Eq. (3) can be neglected, $\varepsilon_{||} \approx -\omega_{pe}{}^2/\omega^2$. With this approximation we find

$$k_z^2 = \frac{\omega^2}{c^2}\varepsilon_{\perp}(1 + k_x^2 \delta_e^2) \tag{8}$$

or

$$\hat{k}_z^2 \equiv \frac{k_z^2 c^2}{\Omega_i^2 (1 + k_x^2 \delta_e^2)} = \frac{\omega^2}{\Omega_i^2}\left(1 - \frac{\omega_{pi}^2/\Omega_i^2}{\omega^2/\Omega_i^2 - 1}\right) \tag{9}$$

where $\delta_e = c/\omega_{pe}$ is the electron skin depth. The plot in Fig. 2 shows the region where the SW is evanescent, i.e. in a band above the cyclotron frequency which broadens at high density. In the region of propagation ($k_z^2 > 0$), the group and phase velocities have the same sign, i.e. the SW is a forward propagating mode with respect to the parallel direction.

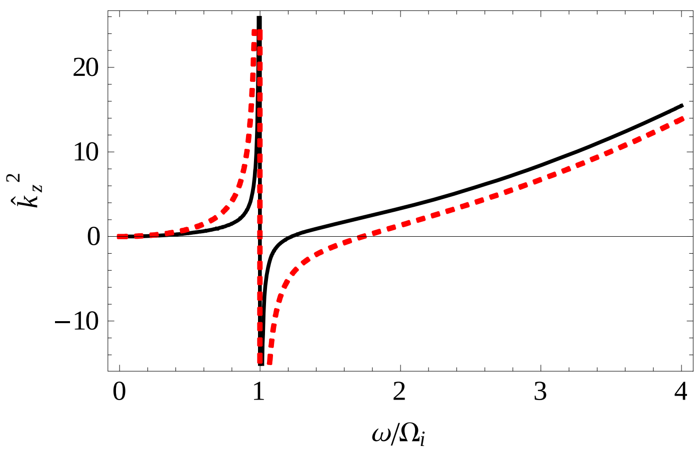

Fig. 2 Dispersion relation of Eq. (9) for ω_{pi}^2/Ω_i^2 = 0.5 (black) and 2.0 (dashed, red).

III. Reflection and absorption at the sheath

The generalized sheath BC is[22]

$$\mathbf{E}_t = \nabla_t\left(\frac{\omega z_s}{4\pi i}\mathbf{s}\cdot\mathbf{D}\right) \tag{10}$$

where z_s is the sheath impedance parameter (the true impedance being $Z = z_s/A_\perp$ with $A_\perp$ the area of the plate), t refers to the tangential direction along the surface, **s** is the unit normal to the surface directed into the plasma, and $\mathbf{D} = \varepsilon\cdot\mathbf{E}$. In the present geometry, $\mathbf{e}_t = \mathbf{e}_x$, $\mathbf{s} = \mathbf{e}_z$, $D_n = \varepsilon_{||}E_z$ and Eq. (10) implies the sheath BC

$$E_x = k_x\frac{\omega z_s}{4\pi}\varepsilon_{||}E_z \tag{11}$$

From Eq. (4) at the sheath, z = 0, we have, for the total fields,

$$E_x = (A+1)(n_x^2 - \varepsilon_{||})/C_{norm} = -(A+1)n_z^2\varepsilon_{||}/(\varepsilon_\perp C_{norm}) \tag{12}$$

$$E_z = (A-1)n_x n_z/C_{norm} \tag{13}$$

where C_{norm} is the normalization factor in the denominator of Eq. (5), the definition of $\mathbf{e}_{sw}$. Combining this with the sheath BC in Eq. (11) and solving for the reflection coefficient A we find

$$A = \frac{\rho - 1}{\rho + 1} \tag{14}$$

where

$$\rho = \frac{\omega z_s k_x^2 \varepsilon_\perp}{4\pi k_z} = \frac{\omega k_x^2 \varepsilon_\perp c_s}{k_z \omega_{pi}^2} \hat{z}_s \tag{15}$$

The compact form of ρ is obtained by using the dispersion relation for the SW. Here, and for future reference, it is convenient to define a dimensionless sheath impedance $\hat{z}_s$ by

$$z_s = \frac{4\pi c_s}{\omega_{pi}^2} \hat{z}_s \tag{16}$$

For $|\rho| \ll 1$ we have $A = -1$ which corresponds to a conducting BC, while for $|\rho| \gg 1$ we have $A = 1$ which is an insulating BC. In both cases, $|A| = 1$, the result is a standing wave, and there is no Poynting flux or power dissipation in the sheath. For complex z_s the Poynting flux and power dissipation are finite and there is a nontrivial change of the complex amplitude of the reflected wave.

The Poynting flux is given by

$$S_z = \frac{c}{16\pi} E_x^* B_y + cc \tag{17}$$

where cc indicates the complex conjugate. For the wave with the usual phase convention $\exp(ik_z z)$, i.e. the A-wave,

$$B_y = n_z E_x - n_x E_z \tag{18}$$

while for the other wave we let $n_z \to -n_z$ in Eq. (18). Using Eqs. (12) and (13) taking account of the sign of n_z for each wave and combining, the total B_y is

$$B_y = (1 - A) n_z \varepsilon_{||} / C_{norm} \tag{19}$$

The Poynting flux may then be expressed in the form

$$S_z = \frac{c}{16\pi} \frac{(|A|^2 - 1 + 2iA_i)}{C_{norm}^2} \frac{n_z^3 \varepsilon_{||}^2}{\varepsilon_\perp} + cc \tag{20}$$

where A_i = Im A, and in applying E_x^* we have used that fact that n_z^2 is always real here, whether the SW is propagating or evanescent. C_{norm} can be related to the amplitude of the $\exp(-ik_z z)$ wave, using Eq. (12),

$$\frac{1}{C_{norm}} \equiv -\frac{\varepsilon_\perp}{n_z^2 \varepsilon_{||}} E_{x0} \tag{21}$$

so that the Poynting flux is

$$S_z = \frac{c}{16\pi}(|A|^2 - 1 + 2iA_i)\frac{\varepsilon_\perp}{n_z}|E_{x0}|^2 + cc \tag{22}$$

From this general expression we can now examine the two cases of interest, propagating and evanescent SWs.

IV. Power absorption for propagating slow waves

For the propagating case, i.e. $\varepsilon_\perp > 0$, n_z is real and the A_i term in Eq. (22) is annihilated. The Poynting flux of the incident and reflected waves are from the -1 and $|A|^2$ terms, respectively.

$$S_z = \frac{c}{8\pi}(|A|^2 - 1)\frac{\varepsilon_\perp}{n_z}|E_{x0}|^2 \tag{23}$$

The fraction of incident power absorbed by the sheath is therefore given by

$$f_P = 1 - |A|^2 \tag{24}$$

Using the dispersion relation, Eq. (7), ρ from Eq. (15) with the dimensionless sheath impedance from Eq. (16) we have

$$\rho = \frac{c_s m_i}{c m_e} \hat{z}_s \varepsilon_\perp^{1/2} \frac{k_x^2 \delta_e^2}{(1 + k_x^2 \delta_e^2)^{1/2}} \equiv \rho_0 e^{i\chi} \tag{25}$$

and

$$|A|^2 = \frac{1 - 2\rho_0 \cos\chi + \rho_0^2}{1 + 2\rho_0 \cos\chi + \rho_0^2} \tag{26}$$

The dependence of f_P on the complex ρ plane is shown in Fig. 3. The largest fractional sheath power absorption occurs for $\rho_0 = 1$ as expected, but significant power absorption also occurs in the general case, and favors $0 \le \chi < 1$ and ρ_0 neither too large nor too small, e.g. in the range $0.2 < \rho_0 < 5$.

For the propagating SW case, χ is just the phase of $\hat{z}_s$. But $\varepsilon_\perp > 0$ implies $\hat{\omega} > (1+\hat{\Omega}^2)^{1/2}$ (where $\hat{\omega} = \omega/\omega_{pi}$ and $\hat{\Omega} = \Omega/\omega_{pi}$). In this sheath regime, the ions are not very mobile,[22] and $\hat{z}_s$ is mostly capacitive, with resistive contributions coming primarily from the electrons. As an example, for $\hat{\omega} = 3$ and $\hat{\Omega} = 1$, the dimensionless sheath impedance is $\hat{z}_s \sim 0.41+1.08i$ (see Table 1 of Ref. 22) which implies $\chi \sim 1.2$. Then estimating $\varepsilon_\perp \sim 1$, $|\hat{z}_s| \sim 1$, $k_x\delta_e \sim 1$, from Eq. (25) $\rho_0 \sim c_s m_i/(c m_e) \sim 0.085\, T_e(\mathrm{eV})^{1/2} \sim 0.4$ at $T_e = 20$ eV and the resulting power absorption fraction is about 40%. Total power absorption in the SW propagating case is not possible: this would require a purely resistive impedance. The capacitive impedance can be small for $\hat{\omega} << 1$ potentially allowing closer proximity to $\rho = 1$ and total absorption, but for ICRF ($\omega > \Omega_i$) this is incompatible with $\varepsilon_\perp > 0$, i.e. $\hat{\omega} > (1+\hat{\Omega}^2)^{1/2}$.

The absolute rf sheath power dissipation per unit area on the surface is obtained from Eq. (23) as $P/A_\perp = -S_z$ which can be rewritten as

$$P/A_\perp\,(\mathrm{MW/m^2}) = 1.33\times 10^{-3}\,\frac{f_P\,\varepsilon_\perp}{n_\parallel}\left|E_{\perp 0}\,(\mathrm{kV/m})\right|^2 \qquad (27)$$

Typically, this dissipation is less than 1 MW/m^2 which should be below the threshold for serious surface damage, but localized heating or global power losses may still be an issue. It tends to be small because, firstly, $0 < f_P < 1$. In the propagating SW regime considered in this section, $\varepsilon_\perp$ is also limited to the range $0 < \varepsilon_\perp < 1$ with 0 pertaining near LH resonance, and 1 under very tenuous plasma conditions. Furthermore, typically $n_\parallel > 1$. In Eq. (27) $E_{\perp 0}$ is the rf electric field amplitude perpendicular to **B** of the incoming wave (as opposed to the total field amplitude at the surface). It is roughly a few kV/m and perhaps as large as a few 10's of kV/m near an ICRF antenna.

V. Power for evanescent slow waves: the sheath plasma resonance

The capacitive limit of the sheath BC gives rise to a well-known phenomenon: the sheath plasma wave (SPW) resonance. This resonance may be viewed as arising from the coupling of the capacitive sheath BC and the inductive plasma response (inductive because $\varepsilon_\parallel < 0$). Here the sheath plasma resonance is considered more generally, for arbitrary sheath impedance. Not surprisingly it is found that the resonance is broadened by dissipation and power can be transferred to the SPW. Power is transferred between two evanescent SW waves, one from the bulk plasma, the other associated with the SPW.

For the evanescent SW case considered in this section, $\varepsilon_\perp < 0$. Taking into account the proper sign for the direction of exponential decay, the appropriate root of the dispersion relation is

$$k_z = -i\frac{\omega}{c}\left|\varepsilon_\perp\right|^{1/2}(1+k_x^2\delta_e^2)^{1/2} \tag{28}$$

$n_z = -i|n_z|$ and Eq. (22) reduces to

$$S_z = \frac{c}{4\pi}A_i\frac{\left|\varepsilon_\perp\right|}{\left|n_z\right|}\left|E_{x0}\right|^2 \tag{29}$$

Note that a single evanescent wave cannot carry a Poynting flux in the direction of the evanescence, but two overlapping evanescent waves can transfer energy between them through a cross-term; this can be considered as evanescent power tunneling. In this case, it does not make sense to discuss incident and reflected waves; rather, the SPW (localized to the sheath region) should be viewed as a resonator with an associated quality factor Q ~ ω (stored energy) / (sheath power dissipation). The power dissipated in the sheath is equal to the power transferred from the A-wave by Eq. (29).

The stored energy is the spatial integral over the SPW fields of the wave energy density[23]

$$u = \frac{1}{32\pi}\left[\mathbf{E}_1^* \cdot \frac{\partial}{\partial\omega}(\omega\bar{\bar{\varepsilon}})\cdot\mathbf{E}_1 + \mathbf{B}_1\cdot\mathbf{B}_1\right] + cc \tag{30}$$

where to avoid confusion with the equilibrium field **B**, subscripts 1 have been added to the wave fields. The stored energy must be calculated in both the explicit plasma region and the implicit Debye scale sheath region. The stored energy in the SPW is derived in the Appendix.

The ρ dependence of the quality factor is inversely proportional to the absorbed power and given by

$$\hat{Q} = -\frac{1}{A_i} = -\frac{1+2\rho_0\cos\chi+\rho_0^2}{2\rho_0\sin\chi} = -\frac{(1+\rho_r)^2+\rho_i^2}{2\rho_i} \tag{31}$$

where $\rho = \rho_r + i\,\rho_i$. For the case at hand, $\varepsilon_\perp < 0$, we have

$$\rho = -i\frac{c_s m_i}{c m_e}\hat{z}_s\left|\varepsilon_\perp\right|^{1/2}\frac{k_x^2\delta_e^2}{(1+k_x^2\delta_e^2)^{1/2}} \equiv \rho_0 e^{i\chi} \tag{32}$$

i.e. $\chi \le 0$ and therefore $A_i \le 0$ so that Eq. (29) implies power is flowing in the negative z direction, i.e. from the A-wave into the SPW. The relation of $\hat{Q}$ to the true oscillator Q is given in the Appendix.

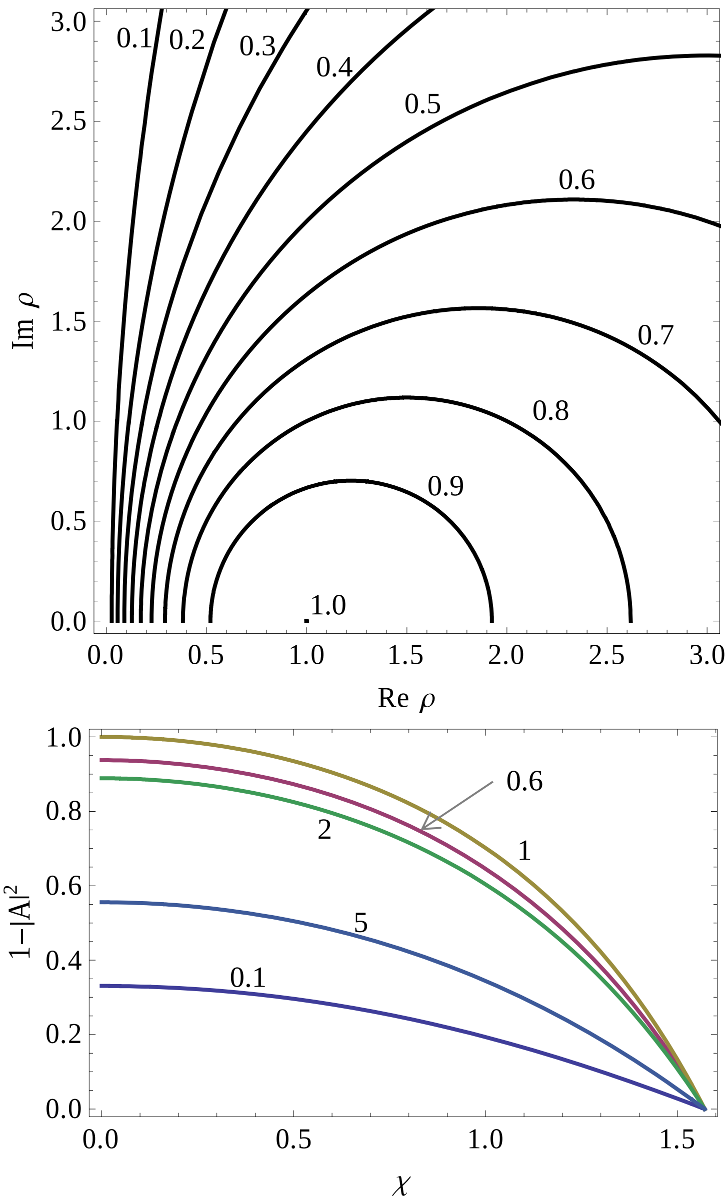

Fig. 3 Upper: contours of P_{sh} fraction in the complex ρ plane; lower: dependence of P_{sh} fraction on phase angle of the impedance for the indicated values of ρ_0. The purely capacitive sheath limit corresponds to $\chi = \pi/2$ and zero power absorption. For negative values of χ or Im ρ (not shown) note that both plots are even about $\chi = 0$.

The resonant case, infinite $\hat{Q}$, occurs for $\chi = A = A_i = 0$ in which case no power flow is needed to sustain the mode at a finite amplitude. The SPW resonance can be recovered from this limit by inserting for $\hat{z}_s$ the capacitive limit $\hat{z}_s = i(\Delta/\omega)(\omega_{pi}/\lambda_d)$. Also in this resonance case, for $A = 0$ we have $\rho = 1$ which from Eq. (28), implies

$$\frac{\omega_{pi}^2}{c}\frac{\Delta}{\omega}|\varepsilon_\perp|^{1/2}\frac{k_x^2\delta_e^2}{(1+k_x^2\delta_e^2)^{1/2}} = 1 \tag{33}$$

Employing Eq. (8) and manipulating

$$ik_z\Delta\varepsilon_{||}\frac{k_x^2\delta_e^2}{(1+k_x^2\delta_e^2)} = -1 \tag{34}$$

This indeed is the condition for SPW resonance, usually quoted in the electrostatic limit $k_x^2\delta_e^2 >> 1$ (See for example Eq. (13) of Ref. 17).

Returning to the case of general sheath impedance, contours of $\hat{Q}$ are shown in Fig. 4. The purely capacitive limit has $\mathrm{Im}\,\rho = 0$ and infinite $\hat{Q}$. With the addition of a resistive component to the sheath impedance, $\mathrm{Im}\,\rho < 0$ and $\hat{Q}$ drops. This implies dissipative resonance broadening due to the sheath power absorption.

Analogous to Eq. (27) the absolute rf sheath power dissipation per unit area on the surface in the case is from Eq. (29)

$$P/A_\perp\,(\mathrm{MW/m^2}) = 2.66\times10^{-3}\left|\frac{\varepsilon_\perp}{\hat{Q}n_{||}}\right||E_{\perp0}\,(\mathrm{kV/m})|^2 \tag{35}$$

i.e. $f_P \rightarrow 2/\hat{Q}$; however, the practical implications are different. Here $E_{\perp0}$ is amplitude of the SPW at the sheath surface (not the total amplitude of all the fields). For the present evanescent SW case, $|\varepsilon_\perp|$ is no longer bounded, but increases with density. Well above the lower-hybrid resonance density, $P/A_\perp$ is proportional to n_e. This can lead to larger dissipation than in the propagating SW case, if $E_{\perp0}$ is large at the wall. Whether this occurs or not will depend on the proximity of the rf source to adjacent limiters.

VI. Discussion and summary

The sample problem considered here illustrates the phenomena of wave reflection, absorption and impedance matching in relation to the generalized sheath boundary condition. The main results of the paper are to be found in Eqs. (15) and (25) which give the dimensionless ratios of wave to sheath impedances ρ for propagating and evanescent slow waves, respectively; and in Eqs. (27) and (35) which give the corresponding rf sheath power dissipation per unit area.

For the SW case examined, and for a perpendicular sheath, the calculation considers two limits. For the propagating SW case, $\varepsilon_\perp > 0$, which requires low plasma density, sheath power absorption can occur for order unity values of ω/ω_{pi} and Ω/ω_{pi} where SW ICRF propagation occurs and the sheath impedance can have a significant real part. For large ω/ω_{pi}, the impedance tends to be dominantly capacitive, and in that case most of the incident SW power is reflected rather than absorbed. Fortunately this, and the fact that $|\varepsilon_\perp| < 1$, constrains the power losses for propagating SWs in the ICRF regime. In the Alfvén wave regime $\omega < \Omega_i$ large sheath power absorption is possible.

For the sheath plasma wave case, corresponds to a localized mode (bound state) near the sheath, the waves are evanescent, $\varepsilon_\perp < 0$, which typically requires high density. There is evanescent tunneling of the power from the plasma wave into the SPW. The SPW resonance can be characterized by a Q which depends on the sheath impedance and plasma parameters. In the high density limit $\omega_{pi} >> \Omega_i$ one can still have $\omega < \omega_{pi}$ implying significant sheath resistance while maintaining $\varepsilon_\perp < 0$ in the ICRF regime, $\omega > \Omega_i$. Thus power transfer to from the SW to the SPW and subsequent sheath dissipation can occur. However, significant sheath dissipation can be avoided if the rf fields evanesce to negligible values before reaching a material surface.

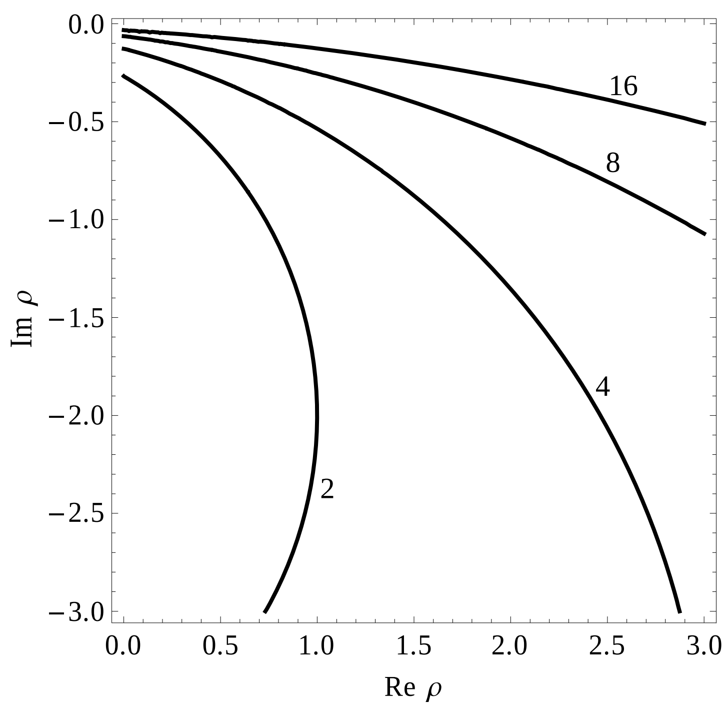

Fig. 4 Contours of normalized resonator quality factor $\hat{Q}$ given by Eq. (31). The plotted quantity is proportional to the conventional Q which also depends on other wave parameters (see Appendix).

Acknowledgements

This material is based upon work supported by the U.S. Department of Energy Office of Science, Office of Fusion Energy Sciences under Award Number DE-FG02-97ER54392. Discussions with H. Kohno and with the RF SciDAC team (Center for Simulation of Wave-Plasma Interactions) are gratefully acknowledged.

Appendix: Stored energy in the sheath plasma wave

For the geometry under consideration we have $\mathbf{k} = (k_x,0,k_z)$, $\mathbf{E} = (E_x,0,E_z)$ and $\mathbf{B}_1 = (0,B_y,0)$ with

$$B_y = \frac{\varepsilon_\perp}{n_z} E_x \tag{A1}$$

$$E_z = \frac{-(\varepsilon_\perp - n_z^2)}{n_x n_z} E_x \tag{A2}$$

Eq. (30), for the SW ordering, gives

$$u_{pl} = \frac{1}{32\pi}\left[\left|B_y\right|^2 + E_x^* \frac{\partial}{\partial\omega}(\omega\varepsilon_\perp)E_x + E_z^* \frac{\partial}{\partial\omega}(\omega\varepsilon_{||})E_z\right] + cc \tag{A3}$$

and expressing all rf fields in terms of E_x results is

$$u_{pl} = \frac{\left|E_x\right|^2}{16\pi}\left[\frac{\varepsilon_\perp^2}{\left|n_z\right|^2} + \frac{\partial}{\partial\omega}(\omega\varepsilon_\perp) + \frac{(\varepsilon_\perp - n_z^2)^2}{n_x^2\left|n_z\right|^2}\frac{\partial}{\partial\omega}(\omega\varepsilon_{||})\right] \tag{A4}$$

where we note that n_z^2 is real (but n_z is not) and the all terms in the brackets in Eq. (A3) are real, hence the complex conjugate (cc) gives a factor of 2. This is the energy density of the SPW on the plasma side of the sheath. The total energy on the plasma side is given by integrating over the volume. The SPW is evanescent, therefore, the integration in the z direction gives a factor $1/|k_z|$ and the total energy on the plasma side per unit area in the x-y plane is

$$\mathcal{E}_{pl} = \frac{1}{|k_z|}\frac{|E_{x0}|^2}{16\pi}\left[\frac{\varepsilon_\perp^2}{|n_z|^2} + \frac{\partial}{\partial\omega}(\omega\varepsilon_\perp) + \frac{(\varepsilon_\perp - n_z^2)^2}{n_x^2|n_z|^2}\frac{\partial}{\partial\omega}(\omega\varepsilon_{||})\right] \tag{A5}$$

where E_{x0} is the amplitude at the sheath-plasma interface.

It remains to compute the energy of the SPW from the fields in the sheath itself. The original expression, Eq. (30), is itself only valid for weakly damped waves, therefore it makes sense to evaluate the sheath terms in the limit of a capacitive sheath. In this case, from the "vacuum gap" sheath model[20] the electric field is in the z direction normal to the wall and has constant magnitude $E_z = \Phi_{sh}/\Delta$ where Φ_{sh} is the sheath voltage at the interface and Δ is the sheath width. But $E_{x0} = ik_x \Phi_{sh}$, therefore

$$u_{sh} = \frac{1}{16\pi}|E_z|^2 = \frac{|E_{x0}|^2}{16\pi}\frac{1}{k_x^2\Delta^2} \tag{A6}$$

The energy from the sheath contribution per unit area in the x-y plane is obtained by multiplying by the sheath width

$$\mathcal{E}_{sh} = \frac{|E_{x0}|^2}{16\pi}\frac{1}{k_x^2\Delta} \tag{A7}$$

Finally

$$\mathcal{E} = \mathcal{E}_{pl} + \mathcal{E}_{sh} \tag{A8}$$

$$\mathcal{E} = \frac{|E_{x0}|^2}{16\pi}\left\{\frac{1}{k_x^2\Delta} + \frac{1}{|k_z|}\left[\frac{\varepsilon_\perp^2}{|n_z|^2} + \frac{\partial}{\partial\omega}(\omega\varepsilon_\perp) + \frac{(\varepsilon_\perp - n_z^2)^2}{n_x^2|n_z|^2}\frac{\partial}{\partial\omega}(\omega\varepsilon_{||})\right]\right\} \tag{A9}$$

The sheath term is comparable to the plasma terms at conditions approximating sheath plasma resonance. For example, in the electrostatic (ES) limit Eq. (A9) reduces to

$$\mathcal{E} = \frac{|E_{x0}|^2}{16\pi}\left\{\frac{1}{k_x^2\Delta} + \frac{1}{|k_z|}\left[\frac{\partial}{\partial\omega}(\omega\varepsilon_\perp) + \frac{|k_z|^2}{k_x^2}\frac{\partial}{\partial\omega}(\omega\varepsilon_{||})\right]\right\} \tag{A10}$$

The $\varepsilon_\perp$ and $\varepsilon_{||}$ terms are comparable from the ES dispersion relation

$$k_x^2\varepsilon_\perp + k_z^2\varepsilon_\| = 0 \tag{A11}$$

and the first and third term in Eq. (A10) are comparable when $\Delta k_z\varepsilon_\| \sim 1$ which is true near the sheath plasma resonance.

We can now relate Q and $\hat{Q}$.

$$Q = \frac{\omega\mathcal{E}}{P_{sh}} \tag{A12}$$

where the power dissipated per unit area, $-S_z$, is given by Eq. (29). Therefore in the ES limit

$$Q = -\frac{|k_z|}{4A_i|\varepsilon_\perp|}\left\{\frac{1}{k_x^2\Delta} + \frac{1}{|k_z|}\left[\frac{\partial}{\partial\omega}(\omega\varepsilon_\perp) + \frac{|k_z|^2}{k_x^2}\frac{\partial}{\partial\omega}(\omega\varepsilon_\|)\right]\right\} \tag{A13}$$

From the main text $\hat{Q} = -1/A_i$ thus we have

$$Q = Q_0\hat{Q} \tag{A14}$$

where

$$Q_0 = \frac{|k_z|}{4|\varepsilon_\perp|}\left\{\frac{1}{k_x^2\Delta} + \frac{1}{|k_z|}\left[\frac{\partial}{\partial\omega}(\omega\varepsilon_\perp) + \frac{|k_z|^2}{k_x^2}\frac{\partial}{\partial\omega}(\omega\varepsilon_\|)\right]\right\} \tag{A15}$$

As a further specialized limit consider the case $\Omega_i << \omega << \omega_{pi}$. In this limit $(\partial/\partial\omega)(\omega\varepsilon_\perp) = \omega_{pi}^2/\omega^2$ and $(\partial/\partial\omega)(\omega\varepsilon_\|) = \omega_{pe}^2/\omega^2$. Using the electrostatic dispersion relation it can be shown that

$$Q_0 = \frac{|k_z|}{4|\varepsilon_\perp|k_x^2}\left(\frac{1}{\Delta} + \frac{2|k_z|\omega_{pe}^2}{\omega^2}\right) \tag{A16}$$

which explicitly shows the comparison between sheath an plasma terms.

References

[1] J.-M. Noterdaeme and G. Van Oost, Plasma Phys. Control. Fusion **35,** 1481 (1993).

[2] J.R. Myra, D.A. D'Ippolito, D.A. Russell, L.A. Berry, E.F. Jaeger and M.D. Carter, Nucl. Fusion **46** S455 (2006).

[3] D. A. D'Ippolito and J. R. Myra, J. Nucl. Mater. **415**, S1001- S1004 (2011).

[4] S. J. Wukitch, M. L. Garrett, R. Ochoukov, J. L. Terry, A. Hubbard, B. Labombard, C. Lau, Y. Lin, B. Lipschultz, D. Miller, M. L. Reinke, D. Whyte, and Alcator C-Mod Team, Phys. Plasmas **20**, 056117 (2013).

[5] V. Bobkov, M. Balden, R. Bilato, F. Braun, R. Dux, A. Herrmann, H. Faugel, H. Fünfgelder, L. Giannone, A. Kallenbach, H. Maier, H.W. Müller, R. Neu, J.-M. Noterdaeme, Th. Pütterich, V. Rohde, N. Tsujii, F. Zeus, H. Zohm and the ASDEX Upgrade Team, Nucl. Fusion **53**, 093018 (2013).

[6] J. Jacquot, D. Milanesio, L. Colas, Y. Corre, M. Goniche, J. Gunn, S. Heuraux, and M. Kubi, Phys. Plasmas **21**, 061509 (2014).

[7] C. M. Qin, Y. P. Zhao, H. Q. Wang, X. J. Zhang, B. N. Wan, J.-M. Noterdaeme, F. Braun, V. Bobkov, H. Kasahara, E. H. Kong, L. Wang, Y. Shuai, Z. X. He, B. J. Ding, ICRF Team and EAST Team, Plasma Phys. Control. Fusion **55**, 015004 (2013).

[8] Y. Corre, M. Firdaouss, L. Colas, A. Argouarch, D. Guilhem, J. Gunn, C Hamlyn-Harris, J. Jacquot, M. Kubic, X. Litaudon, M. Missirlian, M. Richou, G. Ritz, D. Serret and K. Vulliez, Nucl. Fusion **52**, 103010 (2012).

[9] I. Cziegler, J. L. Terry, S. J. Wukitch, M. L. Garrett, C. Lau and Y. Lin, Plasma Phys. Control. Fusion **54**, 105019 (2012).

[10] R.J. Perkins, J.-W. Ahn, R.E. Bell, A. Diallo, S. Gerhardt, T.K. Gray, D.L. Green, E.F. Jaeger, J.C. Hosea, M.A. Jaworski, B.P. LeBlanc, G.J. Kramer, A. McLean, R. Maingi, C.K. Phillips, M. Podesta, L. Roquemore, P.M. Ryan, S. Sabbagh, F. Scotti, G. Taylor and J.R. Wilson, Nucl. Fusion **53**, 083025 (2013).

[11] R. Ochoukov, D. G. Whyte, D. Brunner, D. A. D'Ippolito, B. LaBombard, B. Lipschultz, J. R. Myra, J. L. Terry and S. J. Wukitch, Plasma Phys. Control. Fusion **56**, 015004 (2014).

[12] L. Colas, J. Jacquot, S. Heuraux, E. Faudot, K. Crombé, V. Kyrytsya, J. Hillairet and M. Goniche, Phys. Plasmas **19**, 092505 (2012).

[13] D. N. Smithe, D. A. D'Ippolito, and J. R. Myra, AIP Conference Proceedings **1580**, 89 (2014).

[14] N. Bertelli, E.F. Jaeger, J.C. Hosea, C.K. Phillips, L. Berry, S.P. Gerhardt, D. Green, B. LeBlanc, R.J. Perkins, P.M. Ryan, G. Taylor, E.J. Valeo and J.R. Wilson, Nucl. Fusion **54**, 083004 (2014).

[15] D. Van Eester, K. Crombé and V. Kyrytsya, Plasma Phys. Control. Fusion **55**, 055001 (2013).

[16] J.R. Myra and D.A. D'Ippolito, Plasma Phys. Controlled Fusion **52**, 015003 (2010).

[17] H. Kohno, J. R. Myra, and D. A. D'Ippolito, Phys. Plasmas **19**, 012508 (2012).

[18] D. A. D'Ippolito, J. R. Myra, R. Ochoukov, and D. G. Whyte, Plasma Phys. Control. Fusion **55**, 085001 (2013).

[19] H. Kohno, J. R. Myra, and D. A. D'Ippolito, Phys. Plasmas **20**, 082514 (2013).

[20] D. A. D'Ippolito and J. R. Myra, Phys. Plasmas **13**, 102508 (2006).

[21] E. F. Jaeger, L. A. Berry, J. S. Tolliver, and D. B. Batchelor, Phys. Plasmas **2**, 2597 (1995).

[22] J.R. Myra and D.A. D'Ippolito, Phys. Plasmas **22**, 062507 (2015).

[23] G. Bekefi, *Radiation Processes in Plasmas*, (Wiley, New York, 1966), Eq. (1.43).